Electronic structure of $YbCu_2Ge_2$ studied by soft x-ray angle-resolved photoemission spectroscopy

A. Yasui,[1,*] S.-I. Fujimori,[1] I. Kawasaki,[1] T. Okane,[1] Y. Takeda,[1] Y. Saitoh,[1] H. Yamagami,[1,2] A. Sekiyama,[3] R. Settai,[4] T. D. Matsuda,[5] Y. Haga,[5] and Y. Ōnuki[4,5]

[1]*Condensed Matter Science Division, Japan Atomic Energy Agency, Sayo, Hyogo 679-5148, Japan*

[2]*Department of Physics, Kyoto Sangyo University, Kyoto 603-8555, Japan*

[3]*Division of Materials Physics, Graduate School of Engineering Science, Osaka University, Toyonaka, Osaka 560-8531, Japan*

[4]*Department of Physics, Graduate School of Science, Osaka University, Toyonaka, Osaka 560-004, Japan*

[5]*Advanced Science Research Center, Japan Atomic Energy Agency, Tokai, Ibaraki 319-1195, Japan*

(Received 7 June 2011; revised manuscript received 27 October 2011; published 23 November 2011)

We have measured three-dimensional band structure and Fermi surfaces (FSs) of $YbCu_2Ge_2$, which has recently become recognized as a nearly divalent Yb-based compound, by using soft x-ray angle-resolved photoemission spectroscopy. We clarified that the bands with finite Yb $4f$ contribution cross the Fermi level and are slightly involved in the formation of the FSs, in line with the valence-fluctuating state of $YbCu_2Ge_2$. The obtained valence-band dispersions and the FSs are well explained by a relativistic band-structure calculation based on a local-density-approximation (LDA). These results suggest that the LDA calculation is a good starting point for understanding of the electronic state of $YbCu_2Ge_2$ as well as nearly divalent Yb-based compounds.

DOI: 10.1103/PhysRevB.84.195121 PACS number(s): 71.27.+a, 71.18.+y, 79.60.−i

I. INTRODUCTION

Yb-based heavy Fermion (HF) compounds show various attractive physical phenomena such as the field-induced quantum criticality in $YbRh_2Si_2$[1] or the unconventional superconductivity in β-$YbAlB_4$.[2] HF compounds are characterized by their large electronic specific-heat coefficient γ, which corresponds to the electron effective mass. It has been thought that the formation of the HF states is described as a competition between the Kondo effect and the Ruderman-Kittel-Kasuya-Yosida (RKKY) interaction, and both of them originate from the hybridization between the Yb $4f$ states and the conduction band (c-f hybridization). In order to bring about a comprehensive understanding of the electronic properties of Yb-based HF compounds, it is important to clarify their conduction-band structure including the contribution of the Yb $4f$ electrons. The most essential information is how the $4f$ states are hybridized with the conduction band, and how they are involved in the Fermi surfaces (FSs).

Angle-resolved photoemission spectroscopy (ARPES) is a powerful experimental tool for the study of the electronic structure of materials, since it provides direct information about the valence bands and FSs. Many ARPES studies have been performed for Ce- and U-based HF compounds. Recently, signatures of the HF state have been directly observed by using resonant ARPES for some Ce compounds.[3] In addition, three-dimensional (3D) band structures of various strongly correlated rare-earth and actinide compounds such as $CeRu_2Ge_2$[4] or UB_2[5] have been obtained. On the other hand, for Yb-based compounds, there are only a few ARPES studies on $YbRh_2Si_2$ and $YbIr_2Si_2$.[6] Thus the electronic structure of Yb-based compounds has not been understood yet experimentally. This makes it difficult to establish theoretical pictures of the electronic structure of Yb-based compounds. Therefore, ARPES studies for Yb-based compounds with a wide variety of γ values are needed to understand the HF formation in Yb-based compounds.

We have studied the electronic structure of $YbCu_2Ge_2$ which has a small γ value of 9–10 mJ/(mol K^2). Compounds with small γ value are expected to have a simple electronic structure, therefore $YbCu_2Ge_2$ should be a good starting point to understand the electronic structure of yet poorly studied Yb-based compounds. $YbCu_2Ge_2$ crystallizes in the body-centered tetragonal $ThCr_2Si_2$-type structure. This compound had been considered to belong to the Yb divalent state by the previous experiments, such as various transport and thermodynamic measurements,[7] x-ray absorption spectroscopy (XAS),[8] and NMR measurements.[9] For example, it has a Pauli paramagnetic behavior with a small γ value and no clear Yb^{3+} structure in the XAS spectra. Dung *et al.* claimed that the de Haas–van Alphen (dHvA) frequencies can be explained by a band structure calculation based on a local-density-approximation (LDA) and $4f$ electrons are not related to the FSs.[7] In those studies, however, information on occupied $4f$ states far from the Fermi energy (E_F) has not been obtained. Especially, it has been unclear whether the Yb $4f$ electrons are hybridized with conduction bands, in other words, whether the Yb $4f$ electrons form band states. In our previous study, we reported that soft x-ray (SX) angle-integrated PES spectra of $YbCu_2Ge_2$ have small but clear Yb^{3+} multiplets, suggesting that $YbCu_2Ge_2$ has finite Yb^{3+} contribution.[10] In addition, the "anticrossing" behavior of Yb $4f$ bands was observed in the SX-ARPES spectra. Thus we concluded that the Yb $4f$ electrons form band states through the hybridization with the conduction bands including the Cu $3d$ and Ge $4p$ electrons. On the other hand, clear Fermi edge originating from Yb $4f$ states was not observed in the spectra, and we could not conclude whether the Yb $4f$ electrons have finite contributions to the transport properties.

Most recently, various experiments have suggested that $YbCu_2Ge_2$ is a valence fluctuation compound. Its magnetic susceptibility shows an increasing behavior at temperatures over 600 K,[11] suggesting that this compound has a very high Kondo temperature. Since $YbCu_2Ge_2$ is in the valence fluctuation state, the Yb $4f$ bands should cross the Fermi level somewhere in the $\boldsymbol{k}$ space, and contribute to the formation of FSs.

In the present study we have performed 3D SX-ARPES measurements for $YbCu_2Ge_2$ to determine the bulk

valence-band electronic structure, especially band dispersions and FSs. For Yb-based compounds, this is the first 3D ARPES study, which can be achieved only by utilizing energy tunable light sources such as synchrotron radiation. The obtained spectra are compared with the theoretical results of the LDA calculation to draw out detailed information of the valence bands. In the previous low-energy ARPES studies on Yb-based compounds, incident photon energies of $h\nu_{\rm inc} = 21.2$–100 eV were used, and the large surface contribution was observed just below bulk Yb^{2+} peaks.[6] Moreover, some additional bands, being not in the LDA band calculation, appeared through the hybridization between the surface states and bulk-originated bands. This made it difficult to discuss its bulk electronic structure. By utilizing SX-ARPES, the contribution from the surface states is significantly suppressed, therefore it enables direct comparison of the experimentally obtained spectra with the bulk band dispersion and the FSs predicted from band structure calculations. For example, the recent SX-ARPES spectra for itinerant f-electron compounds, such as UB_2 with $h\nu_{\rm inc} = 450$–500 eV[5] and $CeRu_2Si_2$ with $h\nu_{\rm inc} = 710$–870 eV,[12,13] were well explained by LDA band structure calculation.

II. EXPERIMENT AND CALCULATION

SX-ARPES measurements were performed at the photoemission endstation of the twin-helical undulator beamline BL23SU of SPring-8 equipped with a VG-SCIENTA SES2002 electron analyzer. The energy resolution was set to be about 90 meV with $h\nu_{\rm inc} = 420$–510 eV. Clean sample surface was obtained by cleaving *in situ* along the (001) plane in the base pressure of about 1×10^{-8} Pa. The Brillouin zone (BZ) of the body-centered tetragonal crystal structure is shown in Fig. 1. The value of the inner potential was determined to be 12 eV by measuring the incident photon energy dependence of ARPES spectra, which corresponds to the scan along the plane indicated by blue stripe. Angular scans with an incident photon energy $h\nu_{\rm inc} = 445$ eV were performed along the high-symmetry k_x-k_y plane including the Γ point shown in the red plane. The sample temperature was kept at 20 K because the phonon broadening of ARPES spectra is negligible at this temperature. Oxygen 1s signals, indicating the surface oxidation, were not observed by the core-level scans at $h\nu_{\rm inc} = 800$ eV before and after the SX-ARPES measurements.

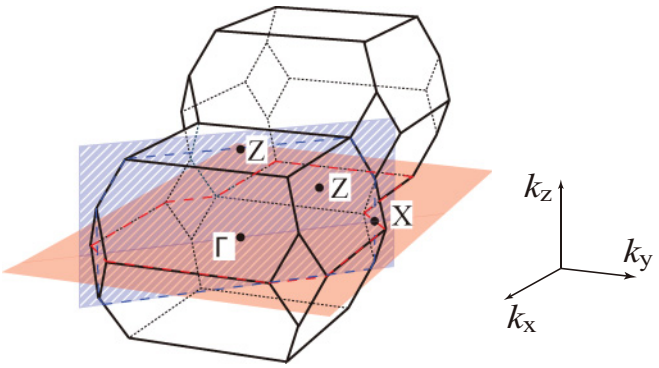

FIG. 1. (Color online) Brillouin zone of body-centered tetragonal structure with indices of the high-symmetry points Γ, Z, and X. Red and blue planes represent the measured region corresponding to the angle-scanning measurement at $h\nu = 445$ eV and the energy-scanning one, respectively.

The theoretical band structure and the FSs of $YbCu_2Ge_2$ were obtained by using a first-principles LDA calculation with the relativistic linearized-augmented-plane-wave (RLAPW) method.[14] This calculation is based on the Dirac one electron equation, so that the spin-orbit (SO) interaction is incorporated into the Hamiltonian without a second variational approximation. In this calculation we used the lattice parameters of $a = 4.0563$ Å, $c = 10.2835$ Å, and $z_{\rm Ge} = 0.38161$ which were determined by the x-ray diffraction experiment.[7] In the self-consistent calculation of the charge density, $4f^{14}$, $6s^2$ electrons at the Yb site, $3d^{10}$, $4s^1$ electrons at the Cu site, and $4s^2$, $4p^2$ electrons at the Ge site are calculated as valence electrons, while the other electrons are treated as core electrons in the relativistic calculations under an atomic-like boundary condition at the APW radii.

III. RESULTS AND DISCUSSION

A. Energy band dispersions

Figure 2(a) shows an intensity plot of the ARPES spectra measured along several high symmetry lines. Each spectrum was normalized with the integrated intensity of energy distribution curve (EDC). The spectra reflect mostly contributions from Yb 4f states and Cu 3d states because the photoionization cross sections (I) of these states are much larger than those of the other states at $h\nu_{\rm inc} = 420$–510 eV, $I_{\rm Yb4}f : I_{\rm Cu3}d : I_{\rm others} \approx 1 : 1/6 : 1/200$ according to atomic calculations.[15] In order to discuss the obtained band structure in more detail, we present theoretical band dispersions together with density of states (DOS) obtained by the LDA calculation in Fig. 2(b). The magnitude of the Yb 4f, the Cu 3d, and the Ge 4p components in each band is represented with a scale of red, blue, and green, respectively. From the DOS it is clear that the valence bands of $YbCu_2Ge_2$ are dominated by the Yb 4f and the Cu 3d electrons.

In Fig. 2(a) two flat bands near $E_{\rm F}$ are the SO split bands of the bulk Yb^{2+} 4f states, whose peak positions are indicated by dashed lines. These bands have been regarded as the structure caused by the final state effects, especially the SO interaction.[6] On the other hand, this structure is reproduced by the RLAPW calculation within the Dirac-based LDA framework in the one-electron ground state. We will discuss the doublet structure in the last part of this section. The Yb^{2+} $4f_{7/2}$ bands just below $E_{\rm F}$ lie at the binding energy $E_{\rm B} = 0.12$ eV, while their SO split counterparts ($4f_{5/2}$ bands) are located on the higher binding energy of $E_{\rm B} = 1.42$ eV. It should be noted that the main part of the Yb^{2+} $4f_{7/2}$ bands is positioned slightly away below $E_{\rm F}$ as has been observed in Yb divalent compounds such as Yb metal or YbS.[16] The SO splitting energy is 1.3 eV, that is almost identical to the calculated one of 1.36 eV. The surface Yb^{2+} 4f bands, which should be located slightly below the bulk Yb^{2+} bands, are not seriously observed compared with the non-4f components in the present SX-ARPES spectra, suggesting that the ARPES data presented in this work reflect the bulk electronic structures. Many dispersive bands are found in the energy region of $E_{\rm B} = 3$–5 eV. They can be

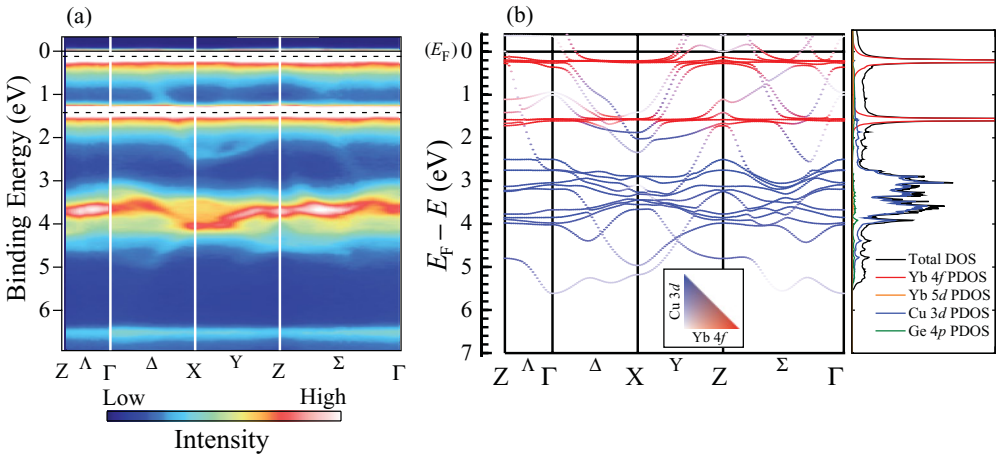

FIG. 2. (Color online) (a) Intensity plot of soft x-ray ARPES spectra along several high symmetry lines. Those spectra were normalized with the integrated intensity of each EDC. The broken lines show peak positions of Yb^{2+} $4f$ bands. (b) Calculated energy band dispersions along high symmetry lines together with density of states. Colors of bands represent projections of Yb $4f$, Cu $3d$, and Ge $4p$ states.

assigned to Cu $3d$ bands, as these are located in the 2.5–5 eV range according to the calculations. The Cu $3d$ bands have stronger dispersions than Yb $4f$ bands. The experimental Cu $3d$ bands correspond to calculated ones, although they are shifted to the lower binding energy side. In addition, there are invisible bands. For example, a hole-like band in the top of Cu $3d$ bands at the Z point is not observed. This mainly comes from the matrix element effect in the photoelectron emission process.[17,18] A flat band located at $E_B = 6.5$ eV is a part of Yb^{3+} multiplet feature which was observed in the angle-integrated photoemission spectrum.[10] This structure cannot be reproduced by the LDA calculation because atomic electronic correlation effects are not taken into account in the LDA framework. Strongly dispersive bands are observed in the energy region of $E_B = 0$–3 eV. Considering their large width, they can be assigned to non-f contributions. In the calculation, the corresponding bands mainly consist of Ge $4p$ and Cu $3d$ states. Therefore, those strongly dispersive non-f bands are conduction bands including the Ge $4p$ and the Cu $3d$ electrons mainly.

Here, we focus on the effect of the c-f hybridization near E_F to understand how the Yb $4f$ states are involved in FSs. Figure 3(a) shows the intensity map of the ARPES spectra in the vicinity of E_F. Figure 3(b) exhibits a comparison between the experimentally determined peak positions and the calculated energy band dispersions. Circles in Fig. 3(b) denote the peak positions derived from the second derivatives of EDCs and momentum distribution curves (MDCs).

The Yb^{2+} $4f_{5/2}$ bands are presented by the bands 15–17 and the $4f_{7/2}$ ones by the bands 21–24. The binding energies of Yb^{2+} $4f$ bands obtained experimentally are almost identical to the calculated energies, although they are shifted to slightly lower binding energies. The dispersive bands in $E_B = 0.5$–1.5 eV are well reproduced by c-f hybridized bands 18–20. However all of the bands predicted by the calculation are not observed experimentally. The strongly hybridized bands 22–24 form FSs in the calculation. In order to show the peak positions of strongly dispersive bands more clearly, we normalized the intensity map surrounded by the pink lines of Fig. 3(a) with integrated intensity of the MDC and show it in Fig. 3(c). In addition, the band positions derived from the MDCs are shown in Fig. 3(d). The experimental bands also have anticrossing features near E_F due to the c-f hybridization. Especially, the anticrossing bands cross the Fermi level in the area around the X point. This means that the Yb $4f$ electrons participate in the formation of FSs through the c-f hybridization, which is not predicted by the dHvA measurement.[7] However, their contributions to FSs are very small as shown in our previous angle-integrated photoemission spectrum.[10] The calculated γ value is 6.46 mJ/(mol K^2), and this is slightly smaller than the experimental value of 9–10 mJ/(mol K^2).[7] This suggests that Yb $4f$ electrons contribute to FSs slightly in the actual system, since the enhancement of the γ value originated from the electron-phonon coupling should be negligible small.[19]

The bands 13–16, which have large contributions from Cu $3d$ states, correspond to the experimental bands located at $E_B = 1.5$–2.5 eV, although there are deviations between the energy positions of the calculated bands and the experimental ones. For example, the experimental bands with its minimum at the X point in $E_B \sim 2.5$ eV are also seen in calculation. Additionally, the bands corresponding to the bands 13 and 14 are experimentally observed along the X–Z and the Z–Γ axes.

B. Fermi surfaces

Figures 4(a) and 4(b) show intensity plots of the integrated ARPES intensities within $E_F \pm 50$ meV. The image in the k_x-k_y plane [Fig. 4(a)] was obtained by fixing incident photon energy to $h\nu_{inc} = 445$ eV and changing photoelectron detection angles. Meanwhile, the image in ($k_x = k_y$)-k_z plane [Fig. 4(b)] was obtained by varying photon energies $h\nu_{inc} = 420$–510 eV. The measured region contains some points with the equivalent symmetry. Thus the k_x-k_y image was constructed from eightfold symmetrizing a triangular region surrounded by the Γ–Z–X line, and ($k_x = k_y$)-k_z image from fourfold symmetrizing a rectangular region done by the Γ–Z–X–X

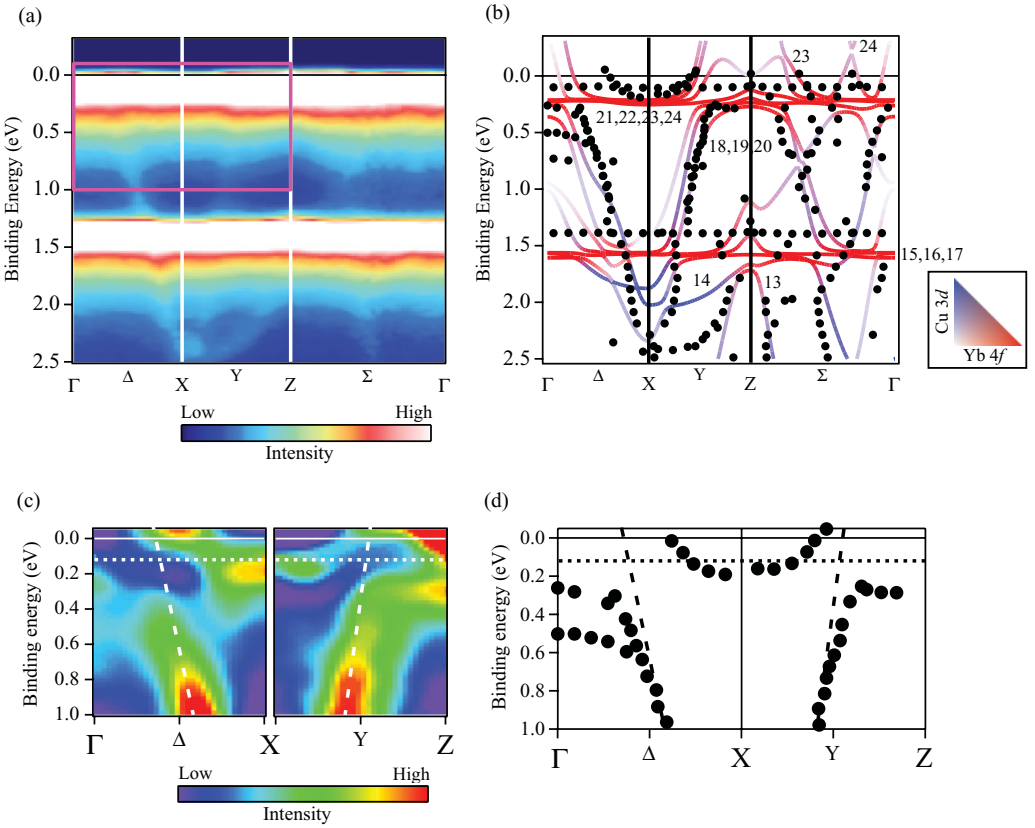

FIG. 3. (Color online) (a) Image plots of SX-ARPES spectra near E_F region. (b) Comparison of the experimentally determined band positions and the calculated energy band dispersions. Filled circles represent the band positions estimated from second derivatives of EDCs and MDCs. Numbers 13–24 represent indices of each calculated energy band. (c) ARPES image normalized with the MDC intensities in the pink rectangular area of (a). The dashed lines are an extrapolation of the dispersive bands below 0.8 eV. The dotted line is the peak position of the Yb^{2+} $4f_{7/2}$ bands. (d) Band positions derived from MDCs. The "anticrossing" behavior created from the c-f hybridization is observed clearly.

line. According to the photoionization cross sections and the energy position of each state, these images represent FSs with large Yb $4f$ contributions. The Fermi momenta determined from the ARPES spectra are plotted with white circles on those figures. For comparison with the experimental data, we show perspective figures of calculated FSs centered at the Γ point, together with the BZ of tetragonal lattice, in Fig. 4(c). The calculated FSs within the k_x-k_y and the $(k_x = k_y)$-k_z planes are shown by red curves in Figs. 4(a) and 4(b), respectively.

In Fig. 4(a) the hexagonal FS stretched along the Γ–X axis corresponds to the quasi-2D electron sheet of the band 24 in the calculation. This FS has a cylindrical shape along the c axis as shown in Fig. 4(b), indicating consistency with the calculation. However, the experimental FS shape is slightly different from the calculated one around the middle point between the Γ and the X points (the Δ axis). This means that the experimentally observed electron FS gets flatter in the $(k_x = k_y)$-k_z plane. The band 24 corresponds to the β branch in the dHvA data.[7] The difference of the FS size between in the experiment and in the calculation was observed also in the dHvA study. The dHvA frequency estimated from our ARPES work is 9.4×10^7–1.0×10^8 Oe, corresponding to the directly obtained value of 9.76×10^7 Oe. The β branch has a little large cyclotron mass of $m_c^* = 3.32m_0$, suggesting that the Yb $4f$ electrons are involved in this FS. This FS has considerably large Yb $4f$ contribution also in the calculation. Its shape might be changed by the electron correlation effect of the Yb $4f$ electrons.

Large diamond-shaped FS is observed around the Z point experimentally as shown in Fig. 4(a). This FS well corresponds to the calculated hole FSs of the bands 22 and 23, although its shape along k_z direction is not clear. The calculated hole FSs have a strong 3D character as shown in Fig. 4(c). This makes it difficult to observe their 3D shapes experimentally within the present momentum resolution along the k_z direction. In addition, the small cyclotron masses were obtained in the corresponding dHvA branches, indicating that those hole FSs have small Yb $4f$ contributions (for example, $m_c^* < 0.5m_0$ in the μ- and o-dHvA branches).[7] Thus, the FS corresponding to the band 23 cannot be detected in Fig. 4(b).

The experimental FS map has a high intensity around the Z point, while there is no FS in the LDA calculation. In the ARPES data shown in Figs. 4(a) and 4(b) there exists a small electron FS. On the other hand, there are hole-like bands below and electron-like bands above E_F around the Z point, but neither of them run through the Fermi level in the calculation. This discrepancy might come from the small deviation of E_F

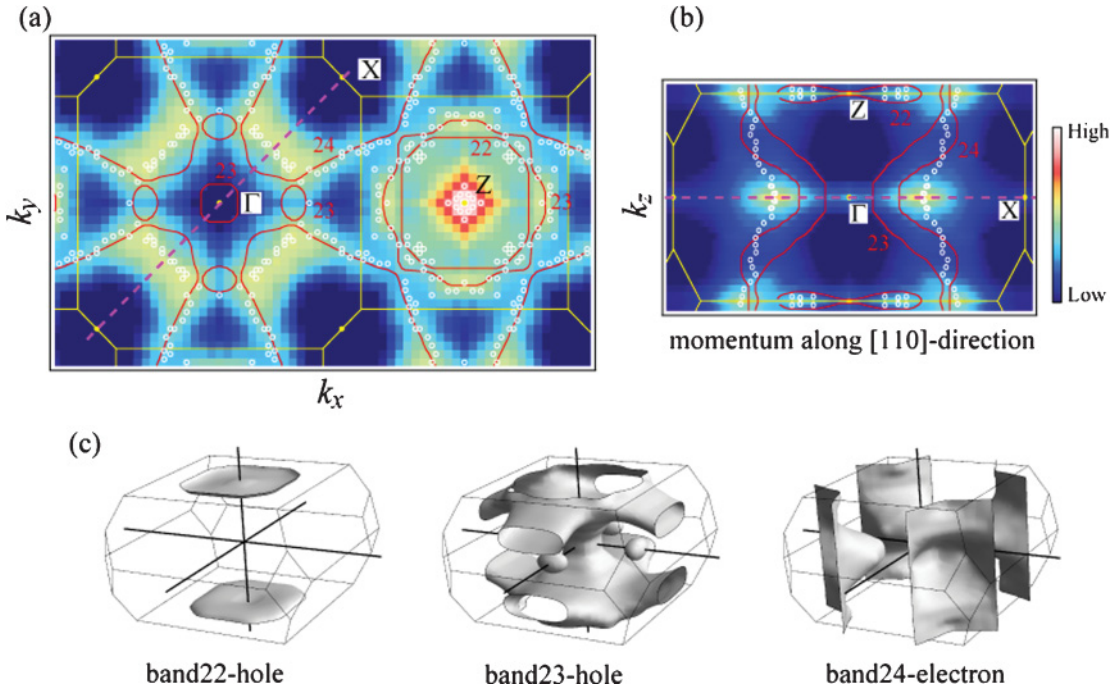

FIG. 4. (Color online) Experimental FSs in the k_x-k_y plane (a) and the ($k_x = k_y$)-k_z plane (b) together with calculated ones. These intensity maps were obtained by integrating the ARPES spectra within $E_F \pm 50$ meV. The yellow lines denote the boundary of body-centered tetragonal BZ. Red curves represent calculated FSs. Pink dashed lines in (a) and (b) indicate the same high symmetry line. (c) Calculated FSs centered at the Γ point. The band 22 and 23 form the hole FSs with strong three-dimensionality, while the band 24 is the electron FS with quasi-two-dimensionality.

between the experiment and the calculation. The band 21 can form the electron FS by small changes of the Fermi level.

To summarize this section, we have found that characteristic features of the energy band dispersions and FSs of $YbCu_2Ge_2$ are explained by the LDA framework as well as other itinerant f-electron compounds such as UB_2[5] and $CeRu_2Si_2$,[12,13] although not all of the bands predicted by the LDA calculation are observed. These results are consistent with the conclusion of the dHvA work by Dung *et al.* in which the LDA calculation could reproduce the experimental dHvA results.[7] Furthermore, they constitute the first direct observation for the Yb $4f$ electrons forming FSs and having delocalized character through the c-f hybridization as seen in the LDA calculation, something which was not achievable by dHvA measurement.

Here we comment on the interpretation of the doublet structure of the Yb^{2+} $4f$ bands. The LDA eigenenergy does not correspond to the total energy of the N-electron system $E(N)$.[20] When the electronic correlation is weak, the energy is approximated by $E(N) - E(N-1)$, which is equal to the one-electron energy observed by the PES. In our experimental data, the observed anticrossing gap width is consistent with the calculated value within the LDA as shown in Fig. 3(b). Thus the effective electronic correlation effects should be small and the LDA calculation well describes the electronic structures near the E_F region of $YbCu_2Ge_2$. In addition, relativistic LDA calculations incorporate the SO interaction in the Hamiltonian without a second variational procedure. Thus we think that the observed doublet structure of the Yb^{2+} $4f$ bands can be accounted for by the one-electron ground state in the relativistic LDA calculation.

In this work we showed how the LDA calculation is suited to the description of the electronic structure of nearly divalent Yb-based compounds. We believe this provides a basis for discussing the electronic structure of Yb-based HF compounds using the band calculations.

IV. CONCLUSION

We have investigated the bulk 3D band structure of $YbCu_2Ge_2$ using the SX-ARPES. We found that the bands with finite contributions from Yb $4f$ states cross E_F and form FSs, which is consistent with recent reports pointing to valence fluctuations in $YbCu_2Ge_2$. The obtained band dispersions and the FSs were reasonably explained by the LDA calculation, including the contribution of each orbital. All these results suggest that the LDA calculation is a good starting point for the understanding of the electronic structure of nearly divalent or weakly valence fluctuating Yb-based compounds. This result is a step forward in the understanding of the electronic structure of Yb-based HF compounds.

ACKNOWLEDGMENTS

The authors wish to thank I. Jarrige for valuable discussions. This work was performed under the Proposal No. 2009B3831 at SPring-8 BL23SU. This work was financially supported by a Grant-in-Aid for Scientific Research on Innovative Areas "Heavy Electrons" (No. 20102003) from the Ministry of Education, Culture, Sports, Science and Technology, Japan.

*a-yasui@spring8.or.jp

[1] P. Gegenwart, J. Custers, C. Geibel, K. Neumaier, T. Tayama, K. Tenya, O. Trovarelli, and F. Steglich, Phys. Rev. Lett. **89**, 056402 (2002).

[2] S. Nakatsuji, K. Kuga, Y. Machida, T. Tayama, T. Sakakibara, Y. Karaki, H. Ishimoto, S. Yonezawa, Y. Maeno, E. Pearson, G. G. Lonzarich, L. Balicas, H. Lee, and Z. Fisk, Nat. Phys. **4**, 603 (2008).

[3] For example, H. J. Im, T. Ito, H.-D. Kim, S. Kimura, K. E. Lee, J. B. Hong, Y. S. Kwon, A. Yasui, and H. Yamagami, Phys. Rev. Lett. **100**, 176402 (2008); A. Koitzsch, S. V. Borisenko, D. Inosov, J. Geck, V. B. Zabolotnyy, H. Shiozawa, M. Knupfer, J. Fink, B. Büchner, E. D. Bauer, J. L. Sarrao, and R. Follath, Phys. Rev. B **77**, 155128 (2008).

[4] M. Yano, A. Sekiyama, H. Fujiwara, T. Saita, S. Imada, T. Muro, Y. Ōnuki, and S. Suga, Phys. Rev. Lett. **98**, 036405 (2007).

[5] T. Ohkochi, S.-I. Fujimori, H. Yamagami, T. Okane, Y. Saitoh, A. Fujimori, Y. Haga, E. Yamamoto, and Y. Ōnuki, Phys. Rev. B **78**, 165110 (2008).

[6] For example, S. Danzenbächer, Yu. Kucherenko, D. V. Vyalikh, M. Holder, C. Laubschat, A. N. Yaresko, C. Krellner, Z. Hossain, C. Geibel, X. J. Zhou, W. L. Yang, N. Mannella, Z. Hussain, Z.-X. Shen, M. Shi, L. Patthey, and S. L. Molodtsov, Phys. Rev. B **75**, 045109 (2007); G. A. Wigger, F. Baumberger, Z.-X. Shen, Z. P. Yin, W. E. Pickett, S. Maquilon, and Z. Fisk, *ibid.* **76**, 035106 (2007).

[7] N. D. Dung, T. D. Matsuda, Y. Haga, S. Ikeda, E. Yamamoto, T. Ishikura, T. Endo, S. Tatsuoka, Y. Aoki, H. Sato, T. Takeuchi, R. Settai, H. Harima, and Y. Ōnuki, J. Phys. Soc. Jpn. **78**, 084711 (2009).

[8] B. D. Padalia, T. K. Hatwar, and M. N. Ghatikar, J. Phys. C **16**, 1537 (1983).

[9] E. V. Sampathkumaran, L. C. Gupta, and R. Vijayaraghavan, J. Phys. C **12**, 4323 (1979).

[10] A. Yasui, S.-I. Fujimori, I. Kawasaki, T. Okane, Y. Takeda, Y. Saitoh, H. Yamagami, A. Sekiyama, R. Settai, T. D. Matsuda, Y. Haga, and Y. Ōnuki, J. Phys. Conf. Ser. **273**, 012067 (2011).

[11] A. Grytsiv, D. Kaczorowski, V.-H. Tran, A. Leithe-Jasper, and P. Rogl, J. Alloys Compd. **504**, 1 (2010).

[12] T. Okane, T. Ohkochi, Y. Takeda, S.-I. Fujimori, A. Yasui, Y. Saitoh, H. Yamagami, A. Fujimori, Y. Matsumoto, M. Sugi, N. Kimura, T. Komatsubara, and H. Aoki, Phys. Rev. Lett. **102**, 216401 (2009).

[13] M. Yano, A. Sekiyama, H. Fujiwara, Y. Amano, S. Imada, T. Muro, M. Yabashi, K. Tamasaku, A. Higashiya, T. Ishikawa, Y. Ōnuki, and S. Suga, Phys. Rev. B **77**, 035118 (2008).

[14] H. Yamagami, J. Phys. Soc. Jpn. **67**, 3176 (1998).

[15] J. J. Yeh and I. Lindau, At. Data Nucl. Data Tables **32**, 1 (1985).

[16] M. Matsunami, A. Chainani, M. Taguchi, R. Eguchi, Y. Ishida, Y. Takata, H. Okamura, T. Nanba, M. Yabashi, K. Tamasaku, Y. Nishino, T. Ishikawa, Y. Senba, H. Ohashi, N. Tsujii, A. Ochiai, and S. Shin, Phys. Rev. B **78**, 195118 (2008).

[17] H. Daimon, S. Imada, H. Nishimoto, and S. Suga, J. Electron Spectrosc. Relat. Phenom. **76**, 487 (1995).

[18] H. Nishimoto, T. Nakatani, T. Matsushita, S. Imada, H. Daimon, and S. Suga, J. Phys. Condens. Matter **8**, 2715 (1996).

[19] The γ value of a non-4f compound YCu_2Si_2, which has the same crystal structure and similar atoms as $YbCu_2Ge_2$, well corresponds to the calculated values [N. D. Dung *et al.*, J. Phys. Soc. Jpn. **77**, 094702 (2008)]. Thus the contribution of the electron-phonon coupling to the γ value should be negligibly small also in $YbCu_2Ge_2$.

[20] According to Janak's theorem [J. F. Janak, Phys. Rev. B **18**, 7165 (1978)], the LDA eigenenergy ϵ_i of the electronic state i corresponds to $\partial E(N)/\partial n_i$, where $E(N)$ is the total energy of the N-electron system and n_i is the occupation number of i state. When the electronic correlation is weak, and thus $\partial\epsilon_i/\partial n_i$ is small, $\partial E(N)/\partial n_i$ is approximated by $E(N) - E(N-1)$.